Small-Molecule Penetrant Diffusion in Hydrocarbon Polymers As Studied by Molecular Dynamics Simulation

Jie Han and Richard H. Boyd*

Department of Materials Science and Engineering and Department of Chemical Engineering, University of Utah, Salt Lake City, Utah 84112

Received April 22, 1994; Revised Manuscript Received June 20, 1994®

ABSTRACT: Molecular dynamics simulations of simple hydrocarbon polymers have been extended to atactic polypropylene (aPP). The equation of state (*PVT*) and the diffusion of methane as a penetrant were studied. The results are compared with previous simulations on the chemically isomeric $(CH_2)_n$ polymers polyethylene (PE) and polyisobutylene (PIB). The equation of state or *PVT* properties are in good agreement with experiment and reproduce the fact that aPP has a melt density similar to that of PE but significantly lower than that for PIB. Small-molecule diffusion in aPP is found to be similar to that in Pe but much faster than that in PIB. This also is in agreement with available experimental data. The molecular packing features that lead to these results are discussed.

I. Introduction

Molecular dynamics (MD) simulations offer the attractive possibility of directly studying time-dependent phenomena in polymeric materials. Unfortunately, the length of time that may be simulated, "the trajectory", is limited by the practical performance in present-day computers to periods of the order of a few nanoseconds. This is far too short for directly studying the time dependence of many properties of interest in polymer technology. However, diffusion of small molecules in polymers seems to be a time-dependent process that does often evolve over this time scale and is thus suitable for MD simulation.

It has been found that, to obtain reliable results for the diffusion coefficients of penetrants in polymeric matrices, it is first very important to demonstrate that the host polymer itself can be simulated reliably.[1,2] Diffusion of the penetrant is very sensitive to free volume in the polymeric medium.[3] Therefore, the volume–pressure–temperature properties of the medium must be relistically represented in simulation. In turn, this means that the nonbonded potential functions used to represent the intermolecular interactions must be well calibrated and capable of reproducing the *PVT* behavior of the polymer host.

In recent work, it has been found that previously existing "united-atom" (UA) nonbonded potential functions for representing the $-CH_2-$ and $-CH_3$ groups in hydrocarbon polymers were not reliable enough to use in diffusion simulations.[1,2] However, it also has been found that a variant of the UA approach can be calibrated so that good *PVT* results for polymers can be obtained.[2,4] The variation involves moving the location at which the potential is centered away from the carbon atoms so that the potential appears to be anisotropic with respect to the latter.[5] The diffusion coefficients for methane in polyethylene (PE) and in polyisobutylene (PIB) from MD simulation were found to be reliable when these "anisotropic" (AUA) potentials were used.[1,2]

In the present work, the availability of calibrated potentials is taken advantage of in studying an interesting situation with respect to the relation between penetrant diffusion and polymer chain structure. The polymers, polyethylene, atactic polypropylene (aPP), and polyisobutylene, are chemically isomeric and have the empirical formula $(CH_2)_n$ (see Figure 1). Yet they differ greatly in their behavior. PIB has a distinctly lower specific volume than PE and, correspondingly, penetrant diffusion is much slower. These observations with respect to PE and PIB have been satisfactorily reproduced in MD simulations.[1,2] The experimental specific volume behavior of aPP is very similar to that of PE. It is therefore of interest to see if simulation can successfully account for this and also to predict the diffusion behavior. In this work we carry out simulations of aPP and compare the results to those for PE and PIB. In previous work, Mueller-Plathe[6] has found the diffusion coefficient for methane in aPP from MD simulation at a single temperature and with the volume fixed at the experimental one. In this work, a number of temperatures are included and the volume is determined by simulation.

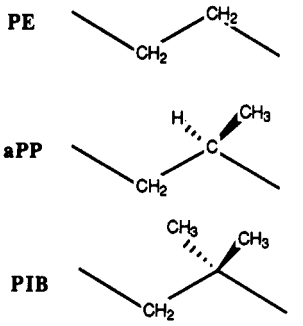

Figure 1. Structures of the three polymers considered.

In previous simulations on PE[4] and PIB,[2] the nonbonded potential functions for the $-CH_2-$ and $-CH_3$ groups were calibrated by adjustment of the parameters to fit *PVT* data. In the present work on aPP, the C and H atoms in the >C–H group were represented explicitly. There are good potentials already available for these atoms,[7] and they can be converted to the "6–12" Lennard-Jones form used here. In fact, this was already done for the >C< atom in PIB.[3] Thus in the present simulations, no new potential functions needed to be calibrated, and the computations are entirely predictive in nature.

II. Simulation Details

The aPP system studied consisted of a single chain of 192 monomer units. The pendent $-CH_3$ groups were placed in random stereosequence, i.e., corresponding to 0.5 replication probability. The $-CH_2-$ and $-CH_3$ groups were represented by "anisotropic" united-atom (AUA) centers whose nonbonded potentials have been previously cali-

® Abstract published in *Advance ACS Abstracts*, August 1, 1994.

0024-9297/94/2227-5365$04.50/0

Table 1. Potential Functions for PP[a]

function	constants	
bond stretch energy = $^1/_2k_R(R - R_0)^2$		
C–C	k_R = 663[b]	R_0 = 1.54
C–H (in >CH–)	k_R = 663[b]	R_0 = 1.09
bond bending energy = $^1/_2k_\theta(\theta - \theta_0)^2$		
$-CH_2-$	k_θ = 482	θ_0 = 111.6°
>C<	k_θ = 482	θ_0 = 109.47°
torsional potential = $^1/_2V_3$ (1 + cos 3ϕ)	V_3 = 13.4	
UA nonbonded potentials, Lennard-Jones 6–12[c]		
$-CH_2-$	ϵ = 0.686	r_{min} = 3.940 σ = 3.510 d = 0.42
>C< (in >CH–)	ϵ = 0.397	R_{min} = 3.872 σ = 3.450 d = 0.0
H (in >CH–)[d]	ϵ = 0.041	R_{min} = 3.37 σ = 3.00 d = 0.0
$-CH_3$	ϵ = 0.837	R_{min} = 4.224 σ = 3.763 d = 0.42
CH_4	ϵ = 1.18	R_{min} = 4.27 σ = 3.80 d = 0.0

[a] Energies in kJ/mol, distances in Å, angles in radians (shown above in degrees). Unless otherwise noted, the potentials are from refs 2 and 4. [b] Lowered by a factor of ~4 from spectroscopic values to increase the MD time step. [c] For the $-CH_2-$ group the potential is of the "AUA" type; the interaction center is offset from the C atom by the distance = d along the bisector of the C–C–C angle in the direction of the hydrogens. The $-CH_3$ potential is also "AUA"; the offset = d is along the C–C bond. [d] From ϵ, R_{min} values in ref 7.

brated.[2,4] The C and H centers of the C–H group were represented explicitly. The parameters of the C···C 6–12 Lennard-Jones potential were found earlier[3] by matching the σ,ϵ values of previously presented "exp-6" potentials.[7] The same procedure was followed here for the H···H potential. The bending and stretching constants are the same as previously employed.[2,4] The C–C stretching constant is attenuated by ~4× over spectroscopic values[7] to increase the time step. The C–H stretching constant is taken the same as for C–C and also represents an attenuation of ~4× over spectroscopic values.[7] All of the parameters are listed in Table 1.

Intramolecular nonbonded interactions were invoked between centers of 1,5 or higher relative displacement but not between 1,4 (or less) centers.

The MD details have been previously described.[2,4] The time step was taken as 0.5 fs, half of the value previously used. This was done in consequence of the lighter explicit H present. Equation of state (*PVT*) data were collected in constant particle number, constant pressure, and constant temperature (*NPT*) runs. The Nosé method was used.[8] The pressure inertial parameter, W, was set to 10^4 atm s^2 m^{-3} and the thermal inertial parameter, Q, was set to 10^{-15} J s^2. The diffusion runs were conducted under effectively *NVT* conditions at volumes established by *NPT* results. Constant V was enforced by a very large inertial parameter W in the *NPT* algorithm.

The dense-packed MD system was initially generated at 500 K from a single isolated chain by placing the latter in a very large periodic box and allowing the volume to decrease at the highest temperature studied in MD runs under *NPT* conditions. Other temperatures were prepared by cooling from higher temperature. The time required for equilibration depended on the temperature. The criteria for equilibration were based on achieving stable volume and energy under *NPT* conditions. Figure 2 shows the volume vs time at a number of the temperatures studied.

In the diffusion studies a single penetrant was used at higher temperatures (350, 375, and 400 K) and four penetrants were used at 300 and 325 K. After equilibration the penetrants were introduced in the periodic box of dimensions determined by the volume equilibration. At the low penetrant concentration involved (1 or 4 particles in 768) the density error involved is minor. The penetrant-containing systems were re-equilibrated for several hundred picoseconds before diffusion data were collected. The diffusion coefficient was determined from one-sixth of the slope of $\langle R_p^2 \rangle$ vs time, where R_p is the distance moved by the penetrant from the t = 0 origin. The averaging implied

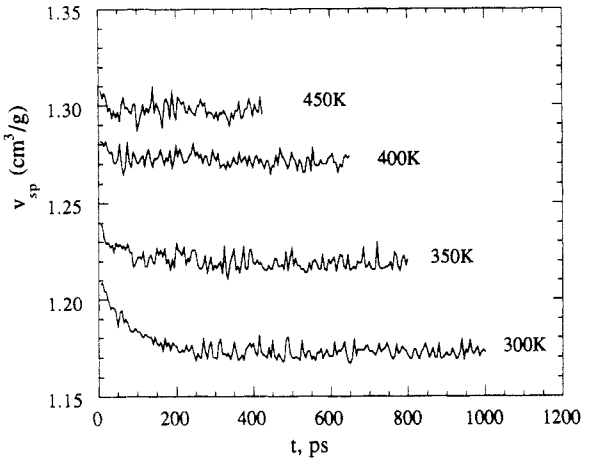

Figure 2. Specific volume of aPP vs time in *NPT* MD simulations at various temperatures. The volumes are 5 ps interval averages.

in $\langle R_p^2 \rangle$ is accomplished by the usual practice of starting new origins (in this case every 1 ps) along the trajectory.[9] The trajectories were continued until the diffusional slope was clearly separable from both the early time cage effect and the later time noise associated with disappearance of multiple trajectories near the end of the run.[2]

It is appropriate to comment on the criteria chosen for the equilibrations. Ideally, a system would be chosen that included a large number of chains, each of which is of high molecular weight. The most stringent equilibration criterion would no doubt be that the centers of mass of the individual *polymer* molecules would undergo displacements larger than the dimensions of the molecules and thus mimic molecular diffusion. Credible attempts have been made to use MD in this domain but only with the considerable simplification of the statistical spring–bead model.[10] These time scales are far beyond the reach of current detailed atomistic simulations. A somewhat less stringent criterion would be that all of the polymer molecule dimensions be equilibrated, including the mean-square end-to-end distance and the radius of gyration. Clarke and co-workers[11] have recently reported a study of 50 and 100 bead chains in the bulk focusing on the equilibration of the molecular dimensions and the effect of starting configurations thereon. They concluded that the nonbonded excluded volume interactions induced a long, molecular weight dependent equilibration time requirement for the molecular dimensions regardless of the preparation method. The requirements of the present work are less stringent yet. It is required that the specific volume of the system be equilibrated and that the local

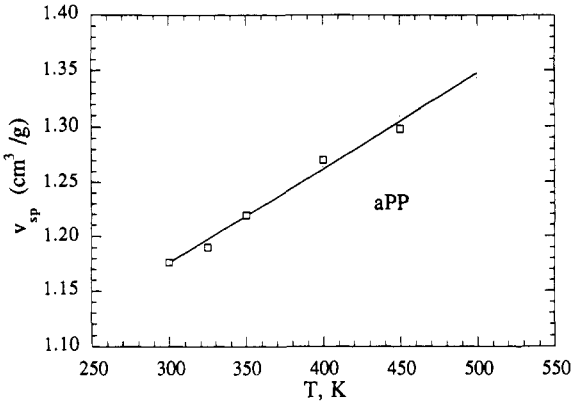

Figure 3. Specific volume (at 1 atm) of aPP vs temperature from MD simulation (points) compared with experiment[12] (solid line).

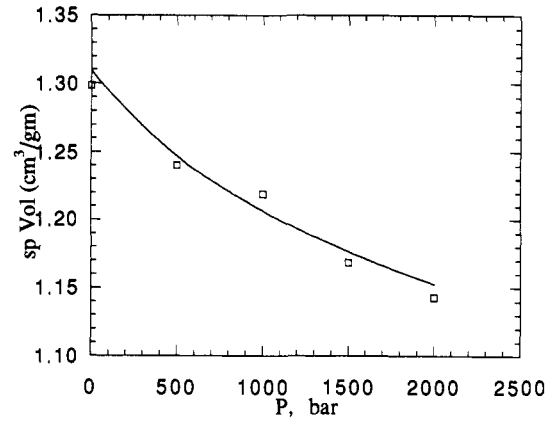

Figure 4. Specific volume (at 450 K) for aPP vs pressure from MD simulation (points) compared with experiment (for iPP, smooth curve[13]).

dynamics be realistic. This is the domain of *segmental* reorientation. In this domain properties such as the glass transition temperature and correlation times for torsional angle, perpendicular dipolar relaxation, and so forth are independent of molecular weight. A measure of this scale would be several *persistence* lengths rather than the overall molecular dimensions. In fact in our model of one chain in a periodic box, overall molecule dimensions are totally lost and only those distances less than half the periodic box size are free from artifacts. From all indications the equilibration times are sufficient to achieve our specific goals.

III. MD Results for the Polymer Host

***PVT* Behavior.** As emphasized above, it is important to represent the *PVT* properties of the host polymer accurately to obtain reliable diffusion results. In the present study, as commented on above, the *PVT* question is of interest in itself. The *V–T* behavior of aPP resulting from *NPT* MD simulations is shown in Figure 3, and *V–P* results are given in Figure 4. Both are compared with experiment.[12,13] The experimental *P–V* data[13] for PP are actually for isotactic polymer (iPP). However, since the *V–T* behavior of molten iPP[12a] and aPP[12b] is virtually identical, it is to be presumed that the melt *V–P* behavior is similar also. It may be seen that the agreement is satisfactory, especially since no new potential function parameters are calibrated.

The *V–T* behavior of aPP is compared with MD[2,4] and experimental[14,15] results for PE and PIB in Figure 5. It may be seen that the MD simulations do a good job of accounting for the specific volumes and their differences

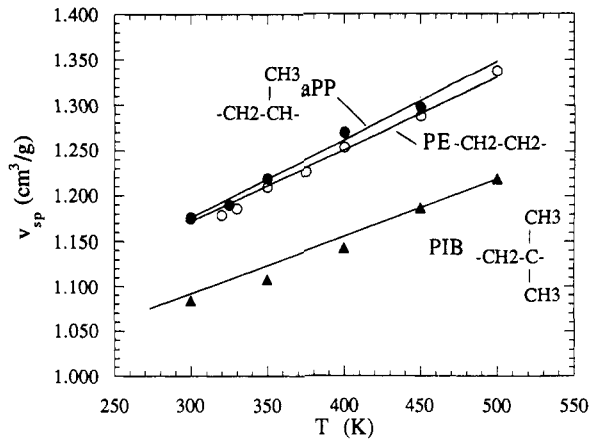

Figure 5. Specific volume vs temperature from MD simulation compared for aPP (this work), PE,[4] and PIB.[2] The solid curves are experiment.[12,14,15]

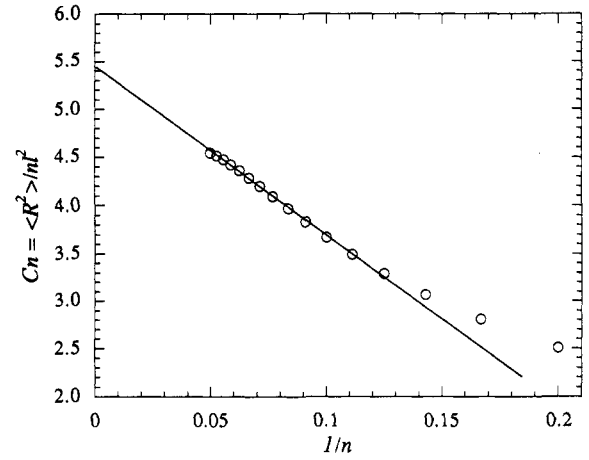

Figure 6. Limiting characteristic ratio of aPP (400 K) determined by extrapolation of $\langle R^2 \rangle / Nl^2$ where N is the chain length and l the bond length vs $1/N$.

due to the chemical structures of the respective polymer chains.

Characteristic Ratio. Another resultant property of the polymer that can be checked against experiment is the characteristic ratio. This is defined[16] as, $C_N = \langle R^2 \rangle / Nl^2$, where $\langle R^2 \rangle$ is the mean-square end-to-end distance, N is the number of bonds, and l is the bond length. Experimental values are available in the high molecular weight limit. As indicated above, in our simulations $\langle R^2 \rangle$ is not meaningful for the entire molecule due to the periodic boundary conditions. However, sufficient shorter distances are available that a credible extrapolation to high molecular weight can be made. Values of R_{ij}^2, where i,j are the indices of main-chain atoms, were computed in the simulations and accumulated according to $N = |i - j|$. These were then used to construct C_N as a function of N. As indicated, because of the periodic boundary conditions, values of $\langle R^2 \rangle^{1/2}$ are reliable only for distances of up to one-half of the periodic box size. Figure 6 shows C_N extrapolated against $1/N$ for values of N consistent with this restriction. Some slight negative curvature due to the periodic boundary condition artifacts is observable in the plot near the point where it was truncated (at $N = 20$). However, the limiting high molecular weight characteristic ratio, C_∞, determined this way seems to be fairly reliable and is 5.4 at 400 K. The experimental value at 418 K is 5.5.[16] The agreement is thus very good, probably to some extent fortuitously so.

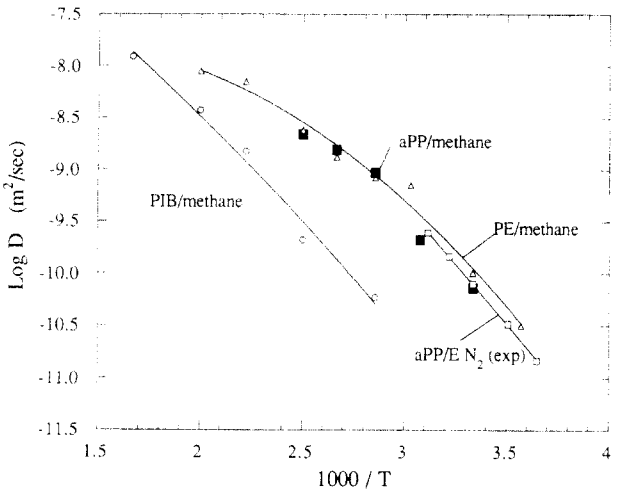

Figure 7. Arrhenius plot of the diffusion coefficient of methane in aPP from MD simulation (filled squares). MD simulation results also are shown for PIB (open circles) and PE in the melt state (open triangles). The curves smooth the MD results for the latter two. Experimental results[17] for nitrogen in EPR rubber (ethylene/propylene copolymer) are shown as open squares.

IV. Diffusion Results

Methane has been chosen as the penetrant for this and previous studies[1,2] because it is the largest molecule and slowest diffuser of the gases commonly studied experimentally. It thus represents a case for testing the ability of MD simulations to be able to computationally generate trajectories long enough to track diffusion. The diffusion coefficients generated for aPP at a number of temperatures are plotted against $1/T$ in Figure 7. The results are compared to those for PE and PIB. As indicated in the Introduction, it was previously shown that for the latter two polymers the MD diffusion results are in agreement with experiment.[1,2]

It may be seen in Figure 7 that the diffusion behavior of methane in aPP is predicted from MD to be very similar to that in PE but very different from that in PIB. This prediction appears to have substance as may be inferred from experimental data for diffusion of nitrogen in ethylene/propylene copolymers (EPR).[17] The latter gas tends to diffuse at a similar but slightly faster rate in comparison to methane.[18] It may be seen that the data for EPR fall near the common relation predicted for methane in the aPP and PE homopolymers.

It is also of interest to compare the details of the diffusion process for aPP with PE and PIB. For PE it was found[2] that the mechanism changes with temperature. At low temperature the process consists of occasional large jumps separated by long time intervals characterized by relatively quiescent cage motion. At high temperature the jumps are very closely spaced in time. The regime of hopping between cages is replaced by a more liquid-like collisional process. The activation energy decreases as temperature increases (Figure 7). In PIB the low-temperature hopping regime is maintained over the whole range displayed in Figure 7. The differences in mechanism are conveniently displayed via a "jump map" where the shorter time cage motion is filtered out.[2] This map is constructed and the filtering accomplished by computing the positional average of the penetrant over a time interval. The difference in average positions between adjacent intervals then defines a jump or lack of one. The time interval is selected wide enough to filter the short time motion but narrow enough that the trajectory of averaged positions gives the same diffusion coefficient as the unfiltered trajectory. Figure 8 shows the jump map for aPP at two temperatures, 300 and 400 K. The 300 K portion shows the hopping regime behavior. Long time intervals between large jumps are apparent. At 400 K the jumps are relatively close together, and the liquid-like regime is approached. As may be seen, the activation energy in Figure 7 also decreases with increasing temperature. Thus aPP behaves much like PE in the details of the jump process as well as in the numerical values of the diffusion coefficient.

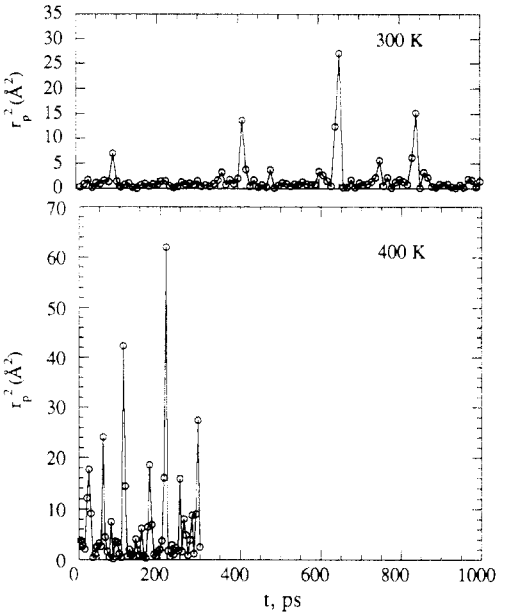

Figure 8. Jump map for a single penetrant in aPP. Upper panel is at 300 K, and the lower one is at 400 K. The squared displacement, r_p^2, is computed between successive 10 ps positional averages of the penetrant at 300 K; at 400 K the interval is 5 ps.

V. Diffusion and Molecular Packing

It is seen above that the penetrant diffusion correlates with the specific volume in the three polymers. That is, the diffusion is markedly slower in the lower specific volume PIB. The concept of free volume is often invoked in rationalizing diffusion. That is, the volume of the system is partitioned as occupied by the molecules and unoccupied free space. The relative ease of diffusion is presumed to be related to the fraction of free space. Further measures of how the free space is parceled in size and shape can also be invoked. In the present work, we have determined the fraction of the system volume available to a probe sphere as a function of the radius of the probe. The criterion for the space being occupied was taken as the space inside of spheres of nonbonded diameter, σ (in Table 1). The position of the occupied sphere was computed from atom coordinates and the AUA offsets, d, in Table 1.

The results of the free volume calculation at 400 K are displayed in Figure 9. The total fractional free volume is the fraction for a sphere of vanishing radius or the $R = 0$ intercept. These values are 0.42 for PE, 0.42 for aPP, and 0.355 for PIB. From these values and the specific volumes of the three polymers (Figure 5), it may be calculated that the *occupied* volumes of the three polymers are 0.74, 0.73, and 0.74 cm³/g, respectively. Thus the *intra*molecular packing efficiencies are virtually identical. Therefore the differences in specific volume and free volume are to be attributed to differing efficiencies of *intermolecular* packing.

In previous work,[3] we have attributed the difference in packing efficiency between PE and PIB to the difference in cross-sectional areas of the chain. Very approximately the chains pack locally as rough or fuzzy cylinders. The

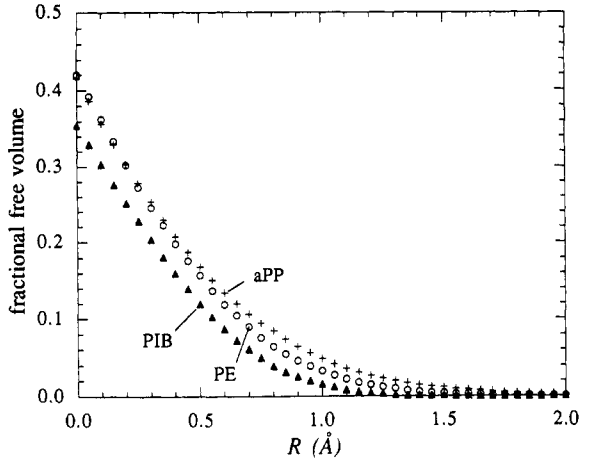

Figure 9. Free volume available to a probe sphere of radius R as a function of sphere radius for PE, aPP, and PIB, at 400 K.

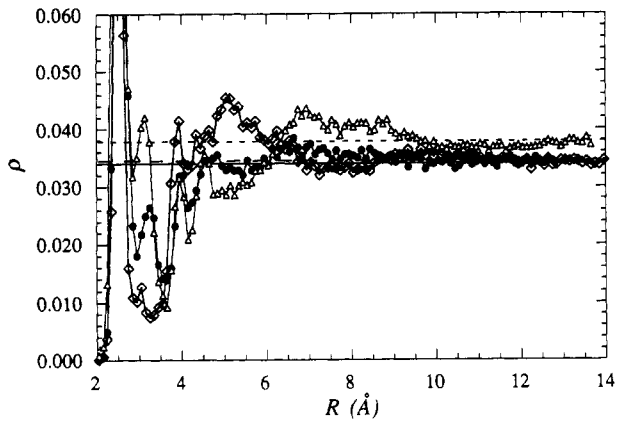

Figure 10. Number density distribution function (centers/Å^3) for PE (diamonds), aPP (filled circles), and PIB (triangles), at 400 K. The average densities are shown as horizontal lines: solid line, PE; long dashes, aPP; short dashes, PIB.

free volume is associated with the surface of these cylinders and is thus proportional to the surface area. The PIB chain has a lower surface to volume ratio than PE because of the thicker cross section occasioned by the pendent methyl groups. Therefore the free volume per carbon atom is smaller in PIB. The aPP case is of course intermediate between PE and PIB with respect to cross-sectional area. Yet the surface roughness which leads to packing deficiencies would presumably be greater than in either PE or PIB.

Further insight into the packing details can be obtained from various distribution functions. Figure 10 shows the complete number distribution function (at 400 K) for the three polymers. This function, $\rho(R)$, is the number density of centers (number/Å^3) at distance R from any given center regardless of type. It is not normalized to unity in order to display the differences in average density. The average densities are shown as horizontal lines. It may be seen that all three arrive at or above the average density by a distance of 6 Å. However, since the intramolecular packing efficiency is the same in the polymers, of more relevance is the intermolecular portion of the number function. The definition of the terms *inter*molecular and *intra*molecular for a single-chain periodic system is illustrated in ref 4. The resultant intermolecular function is displayed in Figure 11. The situation is very different from the complete number function, and the differences in cross-sectional areas are very apparent. In PE the intermolecular function rises quickly to a maximum (at 5.4 Å) characteristic of the interchain spacing of the poorly packed

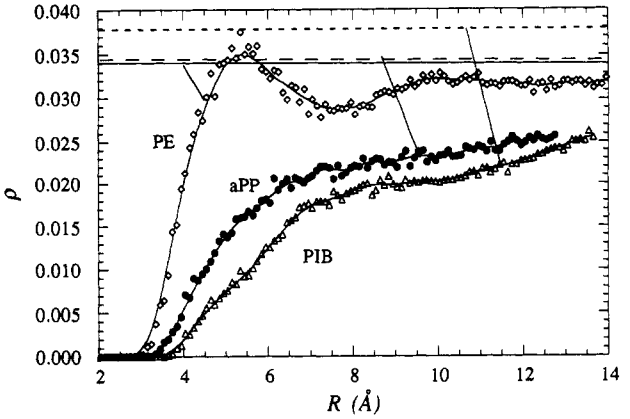

Figure 11. *Inter*molecular contribution to the number density distribution function (centers/Å^3) for PE (diamonds), aPP (filled circles), and PIB (triangles). The average densities are shown as horizontal lines: solid line, PE; long dashes, aPP; short dashes, PIB.

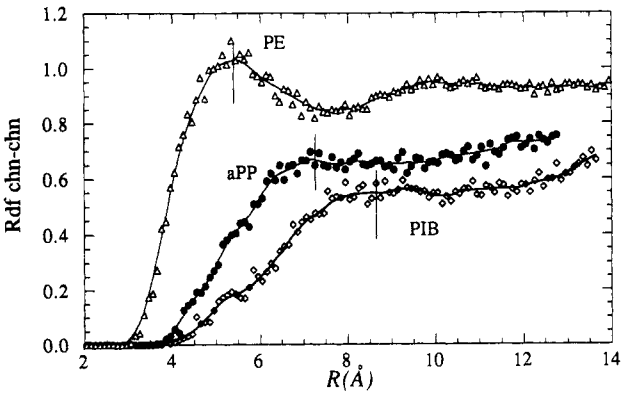

Figure 12. Chain–chain radial distribution function (normalized to unity) based on the distance from any main-chain center to any other main-chain center for PE (diamonds), aPP (filled circles), and PIB (triangles). Approximate interchain spacing is indicated by vertical markers.

cylinders. An "overtone" at approximately twice this distance may even be discerned. For both aPP and PIB the rise is much more gradual, a consequence of the greater cross-sectional areas.

The interchain spacing in PIB and aPP can be discerned somewhat better in a site–site distribution function that includes only main-chain atoms. This is shown in Figure 12, where the function is based on the distances from any main-chain atom to any other main-chain atom. In this case it is normalized to unity. The approximate apparent interchain spacing is indicated by vertical markers. The closest intermolecular contacts or surface to surface contacts are of interest in the context of the thickness of the poorly packed surface layer surrounding the cylinders where the free volume resides. These contacts are seen somewhat better resolved in a site distribution function based on the distance from methyl groups to any other carbon center. Such a display is seen in Figure 13. For aPP a shoulder at ~5.2 Å may be seen and at ~4.8 Å for PIB. Thus the idea of the surface being rougher or more poorly packed in aPP compared to PIB seems to have substance. A close contact methylene–methylene distance is not apparent for PE. However, a very indistinct shoulder or bulge at ~4.5 Å for PE becomes resolved into a separate close contact peak in simulations at lower temperature.[19]

VI. Conclusion

The principal structure–property features discussed in the Introduction seem to be successfully treated by

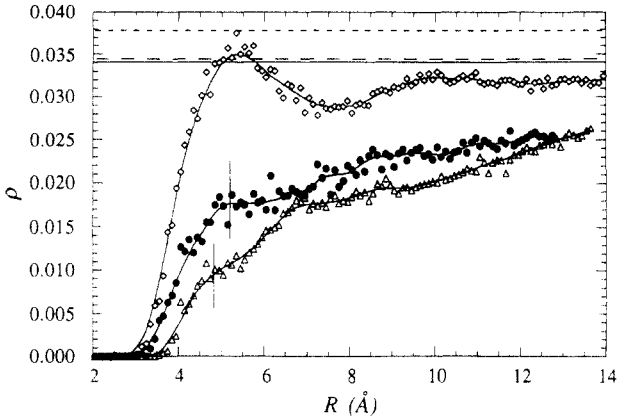

Figure 13. Methyl group *inter*molecular distribution function (400 K) giving the number density of any center (centers/Å^3) at R from pendent methyl groups for aPP (filled circles) and PIB (triangles). The PE (diamonds) *inter*molecular function is also shown. The average densities are shown as horizontal lines: solid line, PE; long dashes, aPP; short dashes, PIB. Vertical markers indicate predominant distance for closest contact of methyl groups with neighboring chain.

simulation. That is, the similarity in *PVT* behavior between PE and aPP, but difference compared to PIB, is reproduced by simulation. In addition, the diffusion behavior is predicted to be very similar in PE and aPP but different in PIB. This also is in agreement with available experimental evidence. Most importantly, it appears that MD simulation holds promise for quantitative predictions of diffusion coefficients.

Acknowledgment. The authors are indebted to the Exxon Chemical Co. (diffusion studies) and to the Polymers Program, Division of Materials Research, National Science Foundation (*PVT* studies), for financial support. The Utah Supercomputing Institute, where the computations were done, is thanked for use of its facilities.

References and Notes

(1) Pant, P. V. K.; Boyd, R. H. *Macromolecules* **1992**, *25*, 494.
(2) Pant, P. V. K.; Boyd, R. H. *Macromolecules* **1993**, *26*, 679.
(3) Boyd, R. H.; Pant, P. V. K. *Macromolecules* **1991**, *24*, 6325.
(4) Pant, P. V. K.; Han, J.; Smith, G. D.; Boyd, R. H. *J. Chem. Phys.* **1993**, *99*, 597.
(5) Toxvaerd, S. *J. Chem. Phys.* **1990**, *93*, 4290.
(6) Mueller-Plathe, F. *J. Chem. Phys.* **1992**, *96*, 3200.
(7) Sorensen, R. A.; Liau, W. B.; Kesner, L.; Boyd, R. H. *Macromolecules* **1988**, *21*, 200.
(8) Nosé, S. *J. Chem. Phys.* **1984**, *81*, 511.
(9) Kremer, K.; Grest, G. S. *J. Chem. Phys.* **1990**, *92*, 5057.
(10) Jolly, D. L.; Bearman, R. J. *Mol. Phys.* **1980**, *41*, 137.
(11) Brown, D.; Clarke, J. H. R.; Okuda, M.; Yamazaki, T. *J. Chem. Phys.* **1994**, *100*, 6011.
(12) (a) Wilski, H. *Kunstoffe* **1964**, *54*, 10. (b) *Ibid.* **1964**, *54*, 90.
(13) Zoller, P. *J. Appl. Polym. Sci.* **1979**, *23*, 1057.
(14) Maloney, D. P.; Prausnitz, J. M. *J. Appl. Polym. Sci.* **1974**, *18*, 2703.
(15) Eichinger, B. E.; Flory, P. J. *Macromolecules* **1968**, *1*, 285.
(16) Boyd, R. H.; Phillips, P. J. *The Science of Polymer Molecules*; Cambridge: New York, 1993; Chapters 6, 7.
(17) Paul, D. R.; Di Benedetto, A. T. *J. Polym. Sci., Part C* **1965**, *10*, 17.
(18) Stannett, V. In *Diffusion in Polymers*; Crank, J., Park, G. S., Eds.; Academic Press: New York, 1968; Chapter 2.
(19) Boyd, R. H.; Pant, P. V. K. *Macromolecules* **1991**, *24*, 4078.